JACS
JOURNAL OF THE AMERICAN CHEMICAL SOCIETY

Communication

pubs.acs.org/JACS

Enhancing the Stability of $CH_3NH_3PbBr_3$ Quantum Dots by Embedding in Silica Spheres Derived from Tetramethyl Orthosilicate in "Waterless" Toluene

Shouqiang Huang, Zhichun Li, Long Kong, Nanwen Zhu, Aidang Shan, and Liang Li*

School of Environmental Science and Engineering, Shanghai Jiao Tong University, 800 Dongchuan Road, Shanghai 200240, China

Supporting Information

ABSTRACT: Methylammonium lead halide perovskites suffer from poor stability because of their high sensitivity to moisture. Inorganic material coatings of SiO_2 are preferred for coupling with perovskites to improve their stability, whereas the conventional SiO_2 formation method is unsuitable because it requires water. Here, a simple SiO_2 generation method based on the high hydrolysis rate of tetramethyl orthosilicate in analytical-grade toluene was developed to avoid the addition of water and catalyst. As a result, SiO_2-encapsulated $CH_3NH_3PbBr_3$ quantum dots (MAPB-QDs/SiO_2) were fabricated without decreasing the quantum yield. Photostability tests indicated that the MAPB-QDs/SiO_2 samples were markedly more stable than the unencapsulated MAPB-QDs. The photoluminescence (PL) of the MAPB-QDs/SiO_2 powders was maintained at 94.10% after 470 nm LED illumination for 7 h, which was much higher than the remnant PL (38.36%) of the pure MAPB-QD sample under a relative humidity of 60%. Similar test results were observed when the MAPB-QDs/SiO_2 powders were incorporated into the poly(methyl methacrylate) films. The enhanced photostability is ascribed to the SiO_2 barriers protecting the MAPB-QDs from degradation.

Methylammonium lead halide perovskites ($CH_3NH_3PbX_3$, X = I, Br, Cl) exhibit excellent optical, excitonic, and charge transport properties and have aroused extensive interest for their application in high-efficiency solar cells.[1] The high photoluminescence (PL) quantum yield and narrow emission band of perovskite quantum dots (QDs) also indicate potential for light-emitting diodes and display applications.[2] However, bulk perovskite materials suffer from poor stability,[3] as do the perovskite QDs with larger surface areas and higher activities. To improve the stability of perovskite solar cells, several materials, including a mesoporous Al_2O_3 buffer layer,[4] vertically aligned TiO_2 nanorods,[5] an NiO_x-ZnO sandwich structure,[6] and reduced graphene oxide,[7] have been introduced to modify the charge transport layers. Although the obtained shelf life of the perovskite solar cells has been extended to thousands of hours, their long-term stability still raises concerns because these methods are not aimed at stabilizing the perovskite itself. Enhancing the stability of the perovskite itself is an alternative for further increasing the service life of the corresponding solar cells and light-emitting diodes.

One major obstacle is that perovskite materials are very sensitive to moisture, and the identification of suitable protective materials to couple with them directly is difficult. The alkylphosphonic acid ω-ammonium chloride has been used to cross-link perovskite crystals,[8] but stable inorganic materials are preferred if possible. The traditional coating material—silica (SiO_2)—is an attractive transparent inorganic material that can protect the core materials against damage due to moisture. SiO_2-coated QDs, e.g., CdSe-SiO_2,[9] CdSe/ZnS-SiO_2,[10] CdSe/CdS/ZnS-SiO_2,[11] and ZnSe-SiO_2,[12] have been widely studied, and their photostabilities have been noted to be dramatically improved after coating. The formation of SiO_2 is commonly based on tetraethyl orthosilicate (TEOS) as a precursor in a controllable mixture containing water, ethanol, (3-mercaptopropyl)-trimethoxysilane (MPS), or ammonia (amines). However, most efforts using these conventional SiO_2 coating methods for perovskite QDs failed because the perovskite QDs are too sensitive to the surrounding environment; the presence of water, alcohols, amines, and even MPS leads to the quenching of the perovskite QDs. The hydrolysis reaction of TEOS is water-assisted, and the formation of SiO_2 layers on perovskite QDs is not possible because the perovskite QDs will be decomposed by water before SiO_2 generation.[13] The development of a method of coating SiO_2 onto perovskite QDs without destroying their PL is a very challenging task.

Here, we report a novel SiO_2 encapsulation process for perovskite QDs; this process is performed in "waterless" toluene, without the addition of any water or catalyst. Toluene was chosen as the solvent for the coating process because of its compatibility with perovskite QDs and its very low-water content (analytical grade, H_2O content 0.0184%). Tetramethyl orthosilicate (TMOS) was used as the precursor because its hydrolysis rate is much faster than that of TEOS,[14] which results in a higher water consumption rate. TMOS enables the formation of SiO_2 layers on perovskite QDs because of the minimal water-driven degradation of perovskite.

Among the perovskite QDs, $CH_3NH_3PbBr_3$ QDs (MAPB-QDs) have attracted increasing attention because of their relatively greater stability than $CH_3NH_3PbI_3$ and $CH_3NH_3PbCl_3$ QDs.[15] Herein, MAPB-QDs were chosen as the core materials to be coated with SiO_2, and the stabilities of the MAPB-QDs/SiO_2 samples were investigated. The synthesis of MAPB-QDs followed a modified ligand-assisted reprecipitation method;[2a] the colloidal

Received: December 15, 2015
Published: April 21, 2016

DOI: 10.1021/jacs.5b13101
J. Am. Chem. Soc. 2016, 138, 5749−5752

solution (the supernatant) with green fluorescence was collected by centrifugation (Figure 1a), and the yellow precipitates at the bottom of the centrifuge tube were discarded. The sharp peaks in the XRD patterns (Figure 1b) indicate that the yellow precipitates are $CH_3NH_3PbBr_3$,[2b,15] and SEM and TEM characterizations (Figure S1) confirm that they are micrometer-sized rods. The colloidal sample exhibits a similar XRD pattern, but its diffraction peaks are broadened, indicating the generation of smaller MAPB crystals. The TEM image further proves that they are MAPB-QDs with an average diameter of 2.4 nm (Figure S2). The high-resolution TEM (HRTEM) images (Figure 1d,e) and the corresponding fast Fourier transform (FFT) pattern (Figure 1f) of MAPB-QDs show the interplanar distances of 2.10 and 1.99 Å, which are consistent with the (022) and (003) crystal faces of $CH_3NH_3PbBr_3$, respectively. The UV–vis absorption and PL emission spectra of the MAPB-QD solution are shown in Figure 1c, and a band edge at 480 nm and a narrow green emission peak at 494 nm are observed for the MAPB-QDs. The green emission has a full-width at half-maximum (fwhm) of 32 nm. The absolute PL quantum yield (PLQY) of MAPB-QDs is measured with an excitation of 450 nm, and a high value of 87% is obtained, which is comparable to that of the previous work.[2b] The fluorescence decay curve (black) of the MAPB-QD solution is shown in Figure S3 with an average lifetime (τ_{avg}) of 16.3 ns (Table S1).

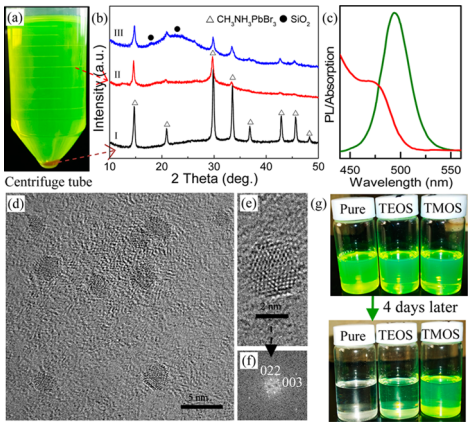

Figure 1. (a) Optical image of the colloidal MAPB-QD solution after centrifugation (illuminated with ambient light). (b) XRD patterns of (I) bulk MAPB precipitates, (II) MAPB-QDs, and (III) MAPB-QDs/SiO_2 (standard encapsulation for 36 h). (c) UV–vis absorption (red line) and PL emission (green line) spectra of the MAPB-QD solution. (d,e) HRTEM images of pure MAPB-QDs and (f) the corresponding FFT pattern. (g) Optical images of the colloidal MAPB-QD solutions with TEOS and TMOS before and after 4 days.

MAPB-QDs exhibit excellent optical properties, but they are very unstable due to their sensitivity to moisture. As shown in Figure 1g, the green light of the pure MAPB-QD solution (0.64 mg/mL) completely disappeared after 4 days in air. In an initial effort to improve the stability of MAPB-QDs, two common silica precursors of TEOS (50 μL) and TMOS (50 μL) were added to 10 mL of the two MAPB-QD solutions (Figure 1g), respectively. After 4 days, the green color of the TEOS-modified sample was substantially weakened. By contrast, the TMOS-modified sample still maintained bright green emission. The addition of TMOS apparently significantly improved the stability of the MAPB-QDs. The differences exhibited by TEOS and TMOS may be associated with their hydrolysis rates. It is conceivable that a very small amount of water was present in toluene (analytical grade), which can initiate the hydrolysis of TEOS and TMOS. Notably, the hydrolysis rate constant of TMOS is more than four times greater than that of TEOS.[14a,16] Thus, most of the water in toluene is consumed faster by TMOS, thereby minimizing the water-driven degradation of MAPB-QDs.

To evaluate the photostability of the MAPB-QD solution improved by TMOS, we designed a test instrument with 450 nm LED illumination. As shown in Figure 2a, two transparent bottom, airtight, quartz colorimetric cuvettes contained 2 mL of the MAPB-QD solutions (0.64 mg/mL), and 10 μL TMOS was added to the solution on the right. Prior to illumination, both solutions were kept in a glovebox (dark environment) for 4 h, and the right-side solution was turned into the MAPB-QDs/SiO_2 solution via hydrolysis of TMOS; the resulting solutions exhibited comparable PLQYs and PL lifetimes (Figure S3 and Table S1). During the first 1–2 h of illumination, enhanced emissions were observed for both solutions (Figure 2b). The PL enhancement is known as the "photoactivation" phenomenon, which originates from the smoothing of MAPB-QDs and the removal of dangling bonds or other surface defects.[17] Upon further illumination, the PL intensities of both samples continuously decreased. However, the PL decay rate of MAPB-QDs was much faster than that of the MAPB-QDs/SiO_2 sample. After 49 h, the remnant PL of the MAPB-QD solution was reduced to 7%, whereas the MAPB-QDs/SiO_2 solution maintained a higher value of 61.03%. The corresponding fwhms (Figure 2c) and PL peak positions (Figure S4) of the MAPB-QDs/SiO_2 solution were located within a narrower range, suggesting that it is more photostable than the MAPB-QD solution. When the two solutions were tested under dark conditions, a similar trend but with slower continuous decrease in PL was observed (Figure S5), and higher humidity led to much faster degradation of the MAPB-QDs. Thus, we inferred that the degradation of MAPB-QDs during the photostability tests is driven by the synergistic effects from the moisture and the illumination. Furthermore, the MAPB-QD solution after two illumination cycles turned to yellow, and some yellow precipitates were formed in the cuvette (Figure 2a), which can well explain the redshifts occurred in the UV–vis absorption spectra (Figure S6). By contrast, the MAPB-QDs/SiO_2 solution after 43 h was still green, and their precipitates on the bottom side were also green. The MAPB-QDs may have been encapsulated by SiO_2, which would have constrained their growth.

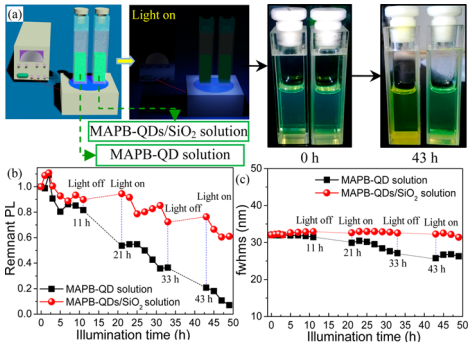

Figure 2. (a) Schematics of the photostability test instrument illuminated with 450 nm LED light (175 mW/cm^2) and the optical images of the cuvettes containing the colloidal MAPB-QD (left) and MAPB-QDs/SiO_2 (right) solutions. (b) Remnant PL emissions and (c) the change in fwhms of the colloidal QD solutions as a function of the illumination time.

DOI: 10.1021/jacs.5b13101
J. Am. Chem. Soc. 2016, 138, 5749–5752

On the basis of the aforementioned observations, a standard SiO_2 encapsulation process was developed for MAPB-QDs in a sealed, three-necked flask with magnetic stirring (to accelerate reaction); this reaction was followed by time-dependent TEM studies. As shown in Figure S7a, 100 μL of TMOS was added to 20 mL of the MAPB-QD solution (0.64 mg/mL) at 25 °C. Figure 3

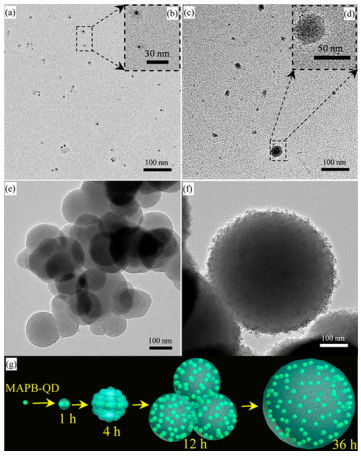

Figure 3. TEM images of MAPB-QDs/SiO_2 with different stirring times: (a,b) 1, (c,d) 4, (e) 12, and (f) 36 h. (g) Schematic of the SiO_2 formation process with increasing stirring time.

shows the TEM images of the obtained MAPB-QDs/SiO_2 samples at different reaction times. After 1 h, amorphous thin SiO_2 layers with thicknesses of several nanometers were coated onto the surface of the MAPB-QDs (Figure 3a,b). When the stirring time reached 4 h, some larger SiO_2 nanoparticles were observed in the TEM image (Figure 3c), and more MAPB-QDs were embedded in these nanoparticles (Figure 3d). For the longer reaction time of 12 h, the SiO_2 nanoparticles grew into spheres (~150 nm), and multiple MAPB-QDs were homogeneously incorporated into the spheres (Figures 3e and S8), whereas some MAPB-QDs were simply attached to the surface of the spheres. After the solution was stirred for 36 h, many green gel precipitates were formed (Figure S7b), which were easily collected by centrifugation (Figure S7c). SEM and TEM images (Figure S9a,b) show that many large SiO_2 spheres with an average size of 470 nm were present in these precipitates; these spheres were perhaps formed through the aggregation of SiO_2 nanoparticles. The HRTEM images (Figure S9c,d) and the corresponding FFT patterns (insets of Figure S9d) confirm that some MAPB-QDs appeared in the outermost surface layer, whereas most of MAPB-QDs were uniformly embedded in the compact SiO_2 spheres (Figure 3f). Thus, the longer stirring time of 36 h was chosen for further experiments. A simple model (Figure 3g) is schematically proposed to explain the aforementioned process. In the initial time, a coating reaction likely occurs (Figure 3a). As the stirring time increases, the MAPB-QDs/SiO_2 grows into large spheres.

To explore the influence of water on the SiO_2 formation process, we investigated open systems directly exposed to RH of 60% and 80% for 1 h; TEM images are shown in Figure S10. Several clusters of MAPB-QDs were observed around the thin SiO_2 layers with the RH of 60% (Figure S10a), and the formed MAPB-QDs/SiO_2 composites were larger than those obtained in the sealed system (Figure 3a). When the RH was increased to 80%, larger numbers of SiO_2 with chain shapes were generated (Figure S10b), and these SiO_2 chains were embedded with MAPB-QDs. The increased moisture content accelerated the hydrolysis of TMOS, but the degradation of MAPB-QDs by water was a serious problem that led to the complete PL quenching of MAPB-QDs (Figure S11). Thus, the sealed system was chosen, in which the SiO_2 generation process is different from those described in the open system.

The XRD pattern of MAPB-QDs/SiO_2 (36 h) is shown in Figure 1b(III). In addition to the $CH_3NH_3PbBr_3$ phase, two weak diffraction peaks of SiO_2 are observed at 17.90° and 23.12°, which correspond to the (010) and ($\bar{1}$01) planes of SiO_2 (PDF Card No. 82-1576). In the survey-scan XPS spectrum of MAPB-QDs/SiO_2 (Figure S12a), enhanced Si and O related peaks clearly appear, and the elements Pb, Br, C, and N are detected with weak signals: the Si 2p peak at 103.5 eV (Figure S12b) and the O 1s peak at 532.9 eV (Figure S12c) is consistent with the binding energies of SiO_2, suggesting the formation of Si−O−Si bonds.[18] Furthermore, in comparison with the FTIR spectrum of MAPB-QDs (Figure S12d), the Si−O−Si bonds generate the most intense peaks at 1073 and 795 cm^{-1} in the spectrum of MAPB-QDs/SiO_2.[19] The peak at 1650 cm^{-1} is assigned to the H−O−H bonds (interlayer water molecule) because of storage in air.[20] The peak at 952 cm^{-1} is assigned to the Si−OH bond, which is generated from the hydrolysis of TMOS.[21]

Figure S13 shows the excitation−emission matrix spectrum of the MAPB-QDs/SiO_2 powders. The PL emission peak at ~505 nm did not change as the excitation wavelength was increased. Compared with the PL peak (494 nm) of the MAPB-QD solution (Figure 1c), the PL redshift may be ascribed to the increased reabsorption of the highly concentrated MAPB-QDs in the MAPB-QDs/SiO_2 powders.[11] The photostabilities of the MAPB-QDs/SiO_2 powders were tested under RH of 60% and 80% (25 °C) by illumination with a 470 nm LED light (21 mW/cm^2), and the instrument is illustrated in Figure S14. In the case of RH 60% (Figure 4a), the remnant PL emission of MAPB-QDs/SiO_2 was

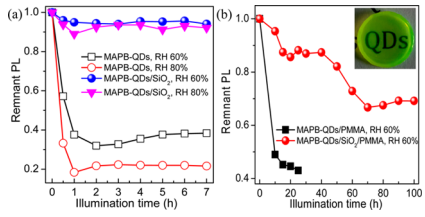

Figure 4. Photostabilities of (a) the MAPB-QD and MAPB-QDs/SiO_2 powders and (b) their films with different RH values under illumination with a 470 nm LED light (inset: optical image of the MAPB-QDs/SiO_2/PMMA film).

94.10% after illumination for 7 h, whereas the value for the MAPB-QDs drastically decreased to 38.36%. For the higher RH of 80%, the MAPB-QDs maintained a smaller remnant PL emission value of 21.63%, indicating that they decomposed faster due to the increased moisture content. By contrast, the MAPB-QDs/SiO_2 powders were not significantly affected by the varied moisture, and a high emission of 92.13% was maintained.

To further explore the application of MAPB-QDs/SiO_2 in display technology, we used them to fabricate hybrid films. The MAPB-QDs are unstable, and many organic binders, such as silicone gel and Norland optical adhesive, are unsuitable because they completely quench the PL of MAPB-QDs. Thus, poly(methyl methacrylate) (PMMA) was selected and dissolved in toluene. After the addition of MAPB-QDs/SiO_2, the resultant mixture was dripped onto a clear glass substrate to form a MAPB-QDs/SiO_2/PMMA film with a diameter of 18 mm and a thickness

DOI: 10.1021/jacs.5b13101
J. Am. Chem. Soc. 2016, 138, 5749−5752

of 1 mm (inset of Figure 4b). As shown in Figure S14, the MAPB-QDs/SiO_2/PMMA film was placed in the sample holder. The photostability was further investigated under continuous 470 nm LED illumination for 100 h (Figure 4b), and the remnant PL emission was 69.16%, followed by the MAPB-QDs/PMMA film with the lower value of 43.01% after 25 h of illumination. As with the pure MAPB-QDs/PMMA film, a part of the loss of luminescence for the MAPB-QDs/SiO_2/PMMA film was caused by the easy degradation of MAPB-QDs embedded in the SiO_2 surface layers, whereas the thicker SiO_2 barriers prevented moisture penetration through PMMA to reach the MAPB-QDs.[11] In comparison with the poor stability of MAPB-QDs, the SiO_2 layers can protect MAPB-QDs (Figure S15) and maintain their high PL emission in LED applications (Figure S16).

To test our TMOS-driven strategy is a universal method to improve the photostability of perovskite QDs, we attempted to use this strategy to generate SiO_2 layers on $CH_3NH_3PbI_3$ QDs (MAPI-QDs), and a similar improvement was observed (Figure S17). Thus, the SiO_2 formation method over TMOS in analytical-grade, "waterless" toluene is practical for the unstable perovskite QDs. Considering the small amount of water (H_2O content 0.0623%) in the toluene solution (Figure S15), ~46% of the water was supplied for the hydrolysis of the TMOS added (100 μL) by toluene. We suspect that some of the required water may originate from the air within the three-necked flask, and the water vapor in the outside air may slowly infiltrate the flask despite the sealing plugs. Furthermore, the small amounts of the added *n*-octylamine, oleic acid, or DMF in toluene may promote the hydrolysis of TMOS, but this reaction can still be performed in pure toluene. We believe that the major factor in controlling the hydrolysis reaction is water.

In summary, we have demonstrated that SiO_2 layers can be formed on perovskite QDs in nonpolar, analytical-grade toluene without the addition of any "harsh" reagents such as alcohols, water, MPS, NaOH or amines, which are usually required for the conventional SiO_2 coating methods but generally lead to quenching of the QDs by damaging their surfaces. Compared with the pure MAPB-QDs, the resulting MAPB-QDs/SiO_2 exhibited improved photostabilities in both solution and powder forms. This improvement is attributed to the hydrolysis of TMOS to rapidly consume water and to the formation of the protective SiO_2 layers. The perovskite QDs and other nanoparticles, including the conventional inorganic QDs synthesized in the organic phase, are generally soluble in nonpolar solvents because of their naturally capping long-chain ligands. Before coating, ligand exchange is an essential step for nanoparticles with hydrophobic surfaces because SiO_2 coatings are usually performed in polar solvents, such as water or alcohols. However, we successfully coated CdSe/CdS QDs and $CuInS_2$/ZnS QDs with SiO_2 in toluene and hexane without ligand exchange. No evident PL quenching behavior was observed for these QDs during the coating process. We believe that this method is a universal SiO_2 encapsulation approach for unstable nanomaterials, especially for nanomaterials that are highly sensitive to moisture.

■ ASSOCIATED CONTENT

Supporting Information

Additional figures and tables. The Supporting Information is available free of charge on the ACS Publications website at DOI: 10.1021/jacs.5b13101.

■ AUTHOR INFORMATION

Corresponding Author

*liangli117@sjtu.edu.cn

Notes

The authors declare no competing financial interest.

■ ACKNOWLEDGMENTS

This work is financially supported by the National Natural Science Foundation of China (NSFC 21271179 and 21436007) and the Program for New Century Excellent Talents (NCET-13-0364).

■ REFERENCES

(1) (a) Yang, W. S.; Noh, J. H.; Jeon, N. J.; Kim, Y. C.; Ryu, S.; Seo, J.; Seok, S. I. *Science* **2015**, *348*, 1234. (b) Ning, Z.; Gong, X.; Comin, R.; Walters, G.; Fan, F.; Voznyy, O.; Yassitepe, E.; Buin, A.; Hoogland, S.; Sargent, E. H. *Nature* **2015**, *523*, 324.

(2) (a) Zhang, F.; Zhong, H.; Chen, C.; Wu, X.; Hu, X.; Huang, H.; Han, J.; Zou, B.; Dong, Y. *ACS Nano* **2015**, *9*, 4533. (b) Huang, H.; Susha, A. S.; Kershaw, S. V.; Hung, T. F.; Rogach, A. L. *Adv. Sci.* **2015**, *2*, 1500194.

(3) Niu, G.; Guo, X.; Wang, L. *J. Mater. Chem. A* **2015**, *3*, 8970.

(4) Guarnera, S.; Abate, A.; Zhang, W.; Foster, J. M.; Richardson, G.; Petrozza, A.; Snaith, H. J. *J. Phys. Chem. Lett.* **2015**, *6*, 432.

(5) Fakharuddin, A.; Di Giacomo, F.; Palma, A. L.; Matteocci, F.; Ahmed, I.; Razza, S.; D'Epifanio, A.; Licoccia, S.; Ismail, J.; Di Carlo, A.; Brown, T. M.; Jose, R. *ACS Nano* **2015**, *9*, 8420.

(6) You, J.; Meng, L.; Song, T. B.; Guo, T. F.; Yang, Y.; Chang, W. H.; Hong, Z.; Chen, H.; Zhou, H.; Chen, Q.; Liu, Y.; De Marco, N.; Yang, Y. *Nat. Nanotechnol.* **2016**, *11*, 75.

(7) Luo, Q.; Zhang, Y.; Liu, C.; Li, J.; Wang, N.; Lin, H. *J. Mater. Chem. A* **2015**, *3*, 15996.

(8) Li, X.; Dar, M. I.; Yi, C.; Luo, J.; Tschumi, M.; Zakeeruddin, S. M.; Nazeeruddin, M. K.; Han, H.; Grätzel, M. *Nat. Chem.* **2015**, *7*, 703.

(9) Selvan, S. T.; Tan, T. T.; Ying, J. Y. *Adv. Mater.* **2005**, *17*, 1620.

(10) Zhang, T.; Stilwell, J. L.; Gerion, D.; Ding, L.; Elboudwarej, O.; Cooke, P. A.; Gray, J. W.; Alivisatos, A. P.; Chen, F. F. *Nano Lett.* **2006**, *6*, 800.

(11) Jun, S.; Lee, J.; Jang, E. *ACS Nano* **2013**, *7*, 1472.

(12) Zhao, B.; Yao, Y.; Gao, M.; Sun, K.; Zhang, J.; Li, W. *Nanoscale* **2015**, *7*, 17231.

(13) (a) Liu, J.; Zhang, L.; Yang, Q.; Li, C. *Microporous Mesoporous Mater.* **2008**, *116*, 330. (b) Yang, J.; Siempelkamp, B. D.; Liu, D.; Kelly, T. L. *ACS Nano* **2015**, *9*, 1955.

(14) (a) Lim, J.; Ha, S. W.; Lee, J. K. *Bull. Korean Chem. Soc.* **2012**, *33*, 1067. (b) Ciriminna, R.; Sciortino, M.; Alonzo, G.; Schrijver, A. D.; Pagliaro, M. *Chem. Rev.* **2011**, *111*, 765.

(15) Schmidt, L. C.; Pertegás, A.; González-Carrero, S.; Malinkiewicz, O.; Agouram, S.; Espallargas, G. M.; Bolink, H. J.; Galian, R. E.; Pérez-Prieto, J. *J. Am. Chem. Soc.* **2014**, *136*, 850.

(16) Chen, K. C.; Tsuchiya, T.; Mackenzie, J. D. *J. Non-Cryst. Solids* **1986**, *81*, 227.

(17) Carrillo-Carrión, C.; Cárdenas, S.; Simonet, B. M.; Valcárcel, M. *Chem. Commun.* **2009**, 5214.

(18) (a) Liu, C.; Yang, D.; Jiao, Y.; Tian, Y.; Wang, Y.; Jiang, Z. *ACS Appl. Mater. Interfaces* **2013**, *5*, 3824. (b) Kim, Y. H.; Lee, D. K.; Cha, H. G.; Kim, C. W.; Kang, Y. S. *J. Phys. Chem. C* **2007**, *111*, 3629.

(19) Bogart, K. H. A.; Dalleska, N. F.; Bogart, G. R.; Fisher, E. R. *J. Vac. Sci. Technol., A* **1995**, *13*, 476.

(20) Kebukawa, Y.; Nakashima, S.; Otsuka, T.; Nakamura-Messenger, K.; Zolensky, M. E. *Meteorit. Planet. Sci.* **2009**, *44*, 545.

(21) Pruthtikul, R.; Liewchirakorn, P. *J. Met., Mater. Miner.* **2008**, *18*, 63.

DOI: 10.1021/jacs.5b13101
J. Am. Chem. Soc. 2016, 138, 5749−5752